Physical Separation in Science and Engineering, 2004,
Vol. 13, No. 1, pp. 1–13

Taylor & Francis
Taylor & Francis Group

MASTER CURVE OF SEPARATION PROCESSES

E. BARSKY[a] and M. BARSKY[b,*]

[a]*Negev Academic College of Engineering, Beer-Sheva, Israel;*
[b]*The Institutes for Applied Research, Ben-Gurion University of the Negev, P.O.B. 653, Beer-Sheva 84105, Israel*

(Received 6 January 2004; In final form 24 February 2004)

Processes of gravity classification involve complex two-phase flows with a multiple-fraction solid phase. Analytic solutions are still lacking for mass processes that comprise solid particles moving in different directions. Consequently, research on gravity classification has been restricted to the study of empirical regularities. This article presents the latest results in this area. Basic to these results is a new physical phenomenon that has been found to apply to the entire class of gravity separation processes – equivalency of the recoveries of the different particulate fractions. In the turbulent zone this regularity is invariant under the main technological factors of the process: flow velocity of the medium, size and density of the particles, density of the medium, concentration of the solid phase. A method has been found for transforming the main process parameters in the laminar and transitional zones to yield identical correlations. This points to the existence of an underlying law governing the process.

Keywords: Efficiency of separation; Particle size; Granulometric composition; Density

1. INTRODUCTION

Gravity classification is very widely used in modern industrial production for classifying pourable materials by particle size, particle density and shape, and other parameters that affect their aerodynamic or hydrodynamic characteristics. Although the first efforts to formulate a theory of the processes involved date back many years [1], it has yet to reach maturity. The reason lies in the exceedingly complex moving medium in which these processes unfold.

Real processes exhibit a wide range of random factors, the most important of which are turbulent eddies of different scales, non-uniformity of the concentration fields, agglomeration of particles within the flow, deviation of particle shapes from the spherical, particle–particle collisions, and particle collisions with the wall of the instrument. These phenomena are easily observed with high-speed cinematography or photography under stroboscopic lighting. The photographs in Fig. 1 show the behaviour of a

*Corresponding author. E-mail: barskym@bgumail.bgu.ac.il

ISSN 1478-6478 print: ISSN 1478-6486 online
DOI: 10.1080/14786470410001685909

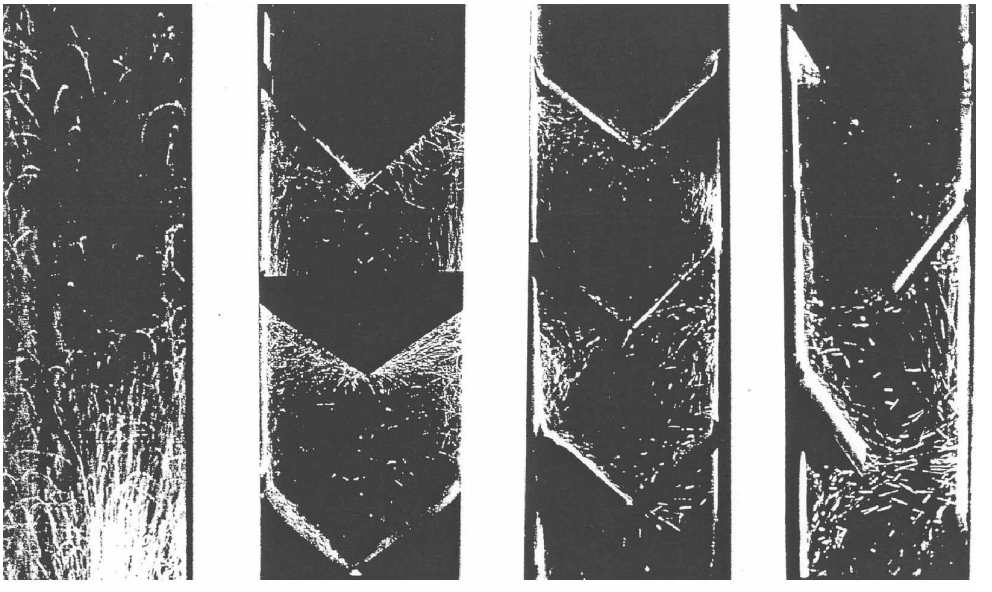

FIGURE 1 Particle motion in different types of classifier.

multi-fraction powder in separation regimes inside channels of four kinds: (a) empty tube; (b) cascade with triangular shelves; (c) cascade with shelves in checker-board array; and (d) cascade with rectangular shelves. As the photographs show clearly, under the influence of the flow and of perturbations, the displacement of each particle is purely random. It is impossible to predict either the instantaneous velocity of the particle or the direction of its displacement, pointing to the presence of elements of chaos in the general picture of the process.

Even in the case of single-phase turbulent flows, which have been extensively studied over the last century, the theory has remained at the level of semi-empirical generalizations [2]. The same can be said of two-phase flows, which are physically more complex. Hence the importance of any regularities or laws discovered by experimentation for the future development of a theory of gravity classification. Over the last few years, we have been engaged in research aimed at shedding light on the main empirical laws that govern gravity classification in a real mass process. Our experiments have been conducted in a variety of instruments differing in cross section and height (Fig. 2). These laws proved to be quite different depending on whether we were looking at the turbulent zone of two-phase flows or the zone of laminar and transitional flow regimes.

2. SEPARATION IN TURBULENT FLOWS

Separation in turbulent air flows is characterized by classifications in which the particle sizes adopted as separation boundary exceed 100 μm. The general results are best

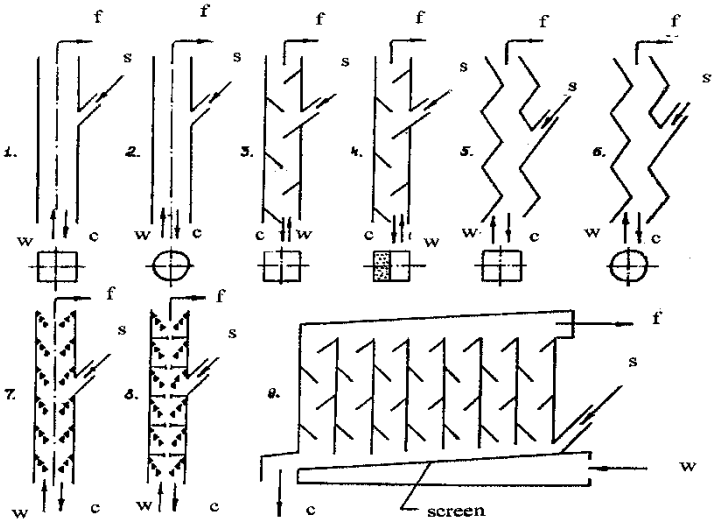

FIGURE 2 Powder classifiers with ascending air flow. Key: 1. Empty tube of square cross-section; 2. Empty tube of circular cross-section; 3. Cascade with plane shelves; 4. Cascade with perforated shelves; 5. Zigzag tube of rectangular cross-section; 6. Zigzag tube of circular cross-section; 7. Multiple cascade; 8. Mutiple cascade with helical inserts; 9. Multiple-column cascade with distribution screen; s – starting material; f – fine product; c – coarse product; w – air velocity.

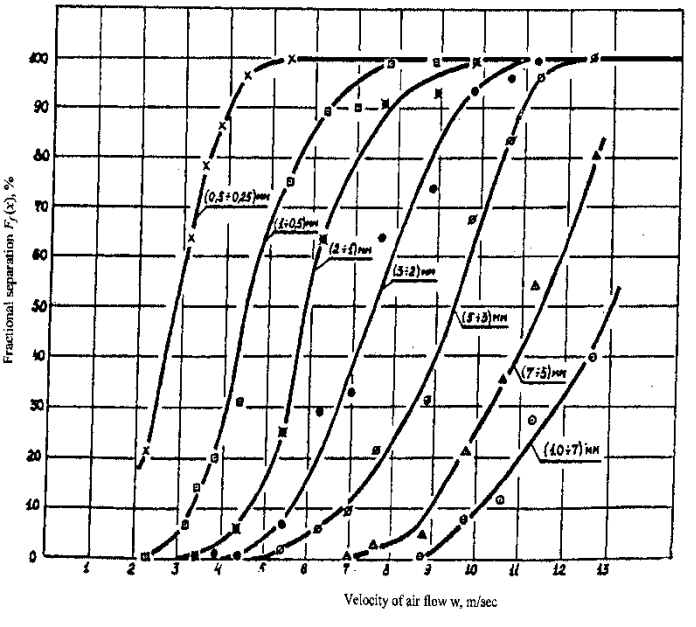

FIGURE 3 Completeness of recovery of particulate fractions of quartzite power as a function of velocity of air flow in cascading shelf air classifier with $z=4$, $i=1$.

illustrated by a concrete example. The curves shown in Fig. 3 were drawn based on experimental findings for the separation of different particulate fractions of pulverized quartzite in a cascading air classifier with four plane shelves ($z=4$); the starting material was introduced onto the uppermost shelf ($i=1$).

Fractional separation is defined as:

$$F_f(x_i) = \frac{n_f(x_i)}{N(x_i)} \cdot 100\% \tag{1}$$

where $N(x_i)$ is the amount of particulate fraction in interval x_i, present in the starting material, and expressed as a fraction or a percentage, while $n_f(x_i)$ is the amount of that fraction present in the fines expressed as a fraction or a percentage, and x_i is the mean size of that particulate fraction.

Here, instead of chaos evidenced in photograph *d* in Fig. 1, the picture is an orderly one (Fig. 3). When there is no ascending current of air all the material drops down; no separation takes place, and thus the degree of separation is zero. At low-flow velocities the finest particles begin to rise while the large particles fall counter to the direction of the flow. As the flow velocity increases even larger particles ascend, with the increase in degree of separation clearly depending on the size of the particles. These relations were characteristic of all gravity classifiers.

An interesting feature of these curves is their invariance in regard to the composition of the starting material, that is, they do not change even when the proportion of the different particulate fractions is varied over a wide range. We verified this observation experimentally in air classifiers by varying the content of the given particular fractions from 3.3 to 95% of the mixture with the other fractions. However, this observation holds only for certain well-defined values of the concentration of solid substance in the carrier medium. The limiting concentrations under which this pattern of invariance holds range from 2 to 8 kg/m^3 depending on the type of instrument involved.

No theoretical explanation of this phenomenon was found. An interpretation became possible only when a statistical theory of the process was developed.

The influence of other parameters is considered to be unpredictable. However, irrespective of the configuration of the channel, we found that in the turbulent flow regimes, the recoveries of different particulate fractions were not only invariant in regard to the composition of the initial feed, they were also identical in form, with the particular coordinates of the separation curve depending solely on the geometry of the channel. This finding holds true for separation boundaries ranging from 100 μm to 10 mm.

Let us illustrate it by considering a concrete example. All the separation curves in Fig. 3 can be transformed into the single curve shown in Fig. 4, when a suitable choice of abscissa is made; for instance when plotting the values of the expression $\mathrm{Fr} = gx/w^2$ on the *x*-axis. Similar results were obtained for all the instruments shown in Fig. 2. This type of their change is called affine transformation. In the above expression, Fr is the non-dimensional Froude number, g is the acceleration of gravity (m/s^2), x is the mean size of particles (m), and w is the velocity of the flow (m/s).

We shall refer to the above expression as the Froude number, as a result of resemblance of this definition and of the classical definition of this number. Its meaning is slightly different, however, since here the linear dimension is that of the particle while the velocity is that of the medium.

This relation was further refined in the course of our investigation of the general features of gravity separation of pourable materials from a mixture of particles of

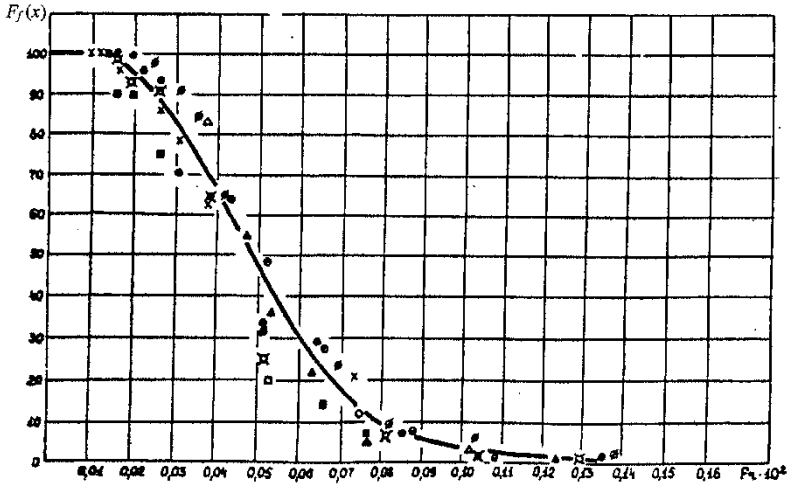

FIGURE 4 Completeness of recovery of particulate fractions of quartzite powder as a function of $\mathrm{Fr} = gx/w^2$ for $z = 4$, $i = 1$.

various densities and sizes. In the most general case the Froude number transforms to parameter B:

$$B = \frac{gx}{w^2} \cdot \frac{(\rho - \rho_o)}{\rho_o}, \tag{2}$$

where ρ and ρ_o are the density of the material and that of the carrier medium (kg/m^3), respectively.

Figure 5 illustrates the dependence of experimentally determined fractional separation yields on B, in the classification of eight types of powder varying in density and grain-size distribution in a cascading shelf classifier ($z = 7$; $i = 2$). The initial granular composition of the powders in terms of successive residues is given in Table I.

Figure 5 shows the experimental values obtained after separation of each of the materials in the classifier, and also of a mixture composed of magnetic iron ore and quartz in different proportions (the choice of materials was dictated by the desire to assure ease of verification of the products, magnetic iron ore being easily separated from quartz using a magnet). Although the experimental points show some degree of scattering, attributable to differences in the shapes of particles in real powders, fluctuations in the velocity of the flow during the experiment, inaccuracies in the granulometric analysis, and so on, the operation of a general regularity is indisputable.

We note that this graph presents the results of nearly three hundred experiments. Analogous results were obtained when other cascading gravity classifiers were tested.

The experimentally and theoretically obtained relation:

$$F_f(x) = \phi(B)$$

proves that, under turbulent regimes of flow of the carrier medium in different kinds of classifiers, the recoveries of the different size and density classes obey a single general law.

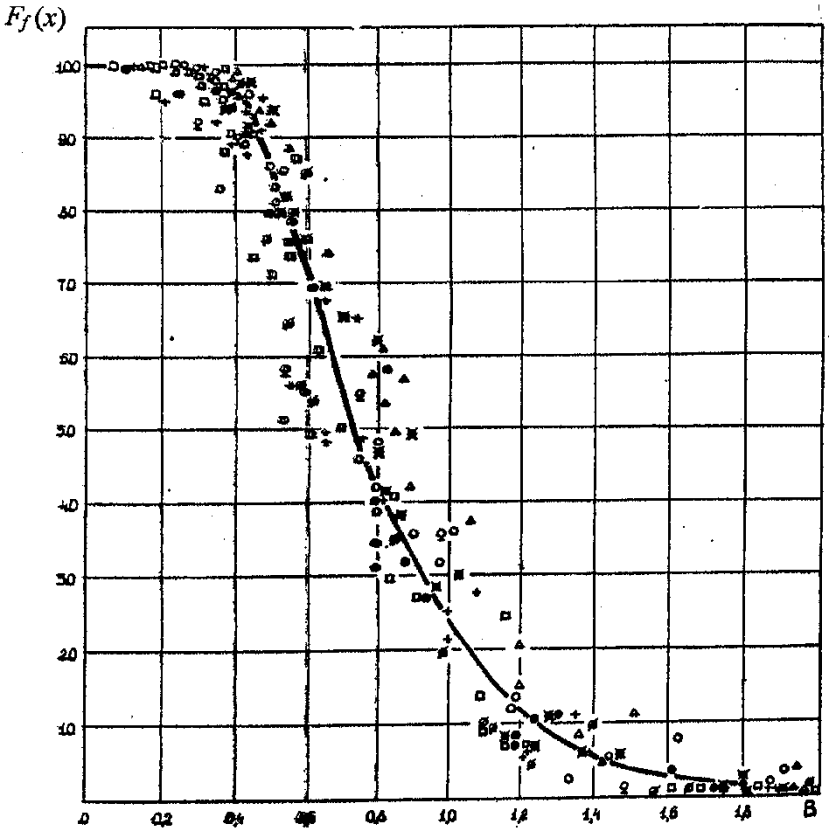

FIGURE 5 Completeness of recovery of particulate fractions of various materials in cascading shelf air classifier with $z=7$, $i=2$ as a function of the expression $B=(gx/w^2)/((\rho-\rho_0)/\rho_0)$. Key: × – granulated polychlorvinyl; ○ – milled quartzite; □ – gypsum gravel; × – granulated cement clinker; + – magnetite; × – granulated alloy No. 1; × – granulated pig iron; ● – granulated alloy No. 2.

TABLE I Initial granular composition of eight types of powdered material

Material	*Density of material* (kg/m)^3	*Successive residues* (%)						
		Mesh size (mm)						
		2.5	*1.5*	*1.0*	*0.75*	*0.43*	*0.20*	*0*
Granulated polychlorvinyl	1070	10.1	20.9	28.5	16.3	15.3	7.97	0.93
Gypsum gravel	1950	13.7	34.1	33.9	5.0	5.3	5.0	3.0
Milled quartzite	2270	4.1	29.5	23.6	10.3	12.9	11.2	8.4
Granulated cement clinker	2675	7.2	27.8	21.2	10.3	15.8	12.8	4.9
Magnetite	3170	0.2	19.4	25.5	11.7	14.5	11.9	16.8
Granulated alloy No. 1	4350	7.2	26.0	22.8	11.3	13.8	13.3	5.6
Granulated pig iron	6210	0.6	10.1	26.8	18.6	25.4	15.2	3.3
Granulated alloy No. 2	*Fine screen*	0.25	0.2	0.15	0.12	0.088	0	–
	$\rho=8650$	12.6	41.8	7.7	7.5	29.7	0.7	–

This law is manifested in the following:

1. Separation of a pourable material in a given instrument proceeds along curves that are identical in shape. It depends neither on the ratio of the particulate fractions in the starting material, nor on the air flow velocity, nor on the concentration (within a working range of 2 to 8 kg/m^3), nor on the density of the starting material, nor on the density of the carrier medium, i.e. there is a universal separation curve that is invariant under all the above parameters. This means that we are dealing with an absolutely deterministic law.
2. As this universal curve is invariant under all the technological parameters listed above, its position in the coordinate system:

$$F_f(x) = \phi(B)$$

reflects only the design of the instrument in which the process was run. This means that it is an indication of the degree of perfection of the design, and hence that different types of classifier should be compared only on the basis of the universal separation curves.
3. The relations that we have found govern all conceivable processes with two-phase flows. According to Fig. 5, in an instrument with $z = 7$, $i = 2$, a falling layer regime prevails at $B > 2.0$, a pneumatic transport regime at $B < 0.2$, while in the $0.2 \leq B \leq 2$ range the separation regimes that incorporates fluidized bed conditions are established as well.
4. In the theory of separation as well as in its practice, considerable effort is devoted to elucidating the optimal separation conditions for particles whose size is identical with the boundary of separation. As is well known, these conditions are met when:

$$F_f(x) = 50\%$$

From the universal curve (Fig. 5) it follows that for any given instrument the optimal conditions are uniquely defined for $B_{50} = \text{const}$. (B_k corresponds to $F_f(x) = k\%$). In addition, with this universal curve, any separation (e.g. $F_f(x) = 20$; 30; 60; 70%; and so on) is uniquely defined by constant B_{20}; B_{30}; B_{60}; B_{70}; and so forth.

It seems puzzling that classification – a chaotic process involving a vast number of particles of irregular form differing in size and density and subject to numerous random factors – should in the end obey a rigorously deterministic law. Let us attempt to clarify the physics of this phenomenon.

According to modern theoretical ideas, for an optimum separation of particles whose size is identical to the boundary of separation, it is necessary that the velocity of the flow is equal to the hovering velocity of the particles. For such a particle the force of gravity will then be equal to the force of dynamic action of the medium:

$$\frac{\pi x_{50}^3}{6} g(\rho - \rho_o) = \lambda_{50} \frac{\pi x_{50}^2}{4} \rho_o \frac{w^2}{2}$$

where x_{50} is size at the separation boundary, at which the particles are extracted in both outlets in equal ratios (the optimum regime), λ is the coefficient of particle resistance in

the medium under the separation conditions, ρ is the material density, and ρ_o is the medium density.

Hence:

$$\mathrm{Fr}_{50}\frac{\rho-\rho_o}{\rho_o}=\frac{3}{4}\lambda_{50}$$

or, taking into account Eq. (2):

$$B_{50}=\frac{3}{4}\lambda_{50} \tag{3}$$

where Fr_{50} and B_{50} are parameters at which the optimal separation takes place.

It follows from Eq. (3) that the parameter B_{50} represents a coefficient of resistance of those particles participating in the mass process in the channel of a given geometry whose size is identical to the boundary of separation. If we assign to this expression the constant value that corresponds to B_{50} for a given instrument, then it is possible to determine the flow regimes from that value that will assure separation of any size or density class with a yield of 50% at each outlet. It is, therefore, possible to carry out the separation process in a way that is optimal for that class.

From the standpoint of the physics of the process, this experimental fact can be interpreted as follows: in any given classifier, any class of identical particles (identical in size and density) will report with equal probability to either of the two outlets when their coefficients of resistance are equal to a certain value that corresponds to the value of B_{50}, characteristic of that instrument.

The fact that the parameter B_{50} is indeed linked to the coefficient of resistance of the particles in a hovering state, is confirmed by the experimentally obtained relation (see Fig. 8):

$$B_{50}=f(\mathrm{Re}_{50})$$

where Re is the Reynolds number. This relationship holds in the entire range of the two-phase flow, in the turbulent as well as in the laminar zones, as will be discussed later.

In other sub-optimal regimes, the particle velocity is governed by the difference between the flow velocity and the hovering velocity of the particle:

$$v=w-w_{50} \tag{4}$$

where v is the velocity of the particle, w is the velocity of the flow, and w_{50} is the velocity of equal separation of class of particles obtained in both outlets.

It follows from Eq. (4) that $w=w_{50}+v$.

The general expression for the parameter B is then given by:

$$B=\frac{qx}{w^2}\cdot\frac{(\rho-\rho_o)}{\rho_o}=\frac{3}{4}\lambda$$

while for the conditions of hovering:

$$B_{50}=\frac{qx}{w^2}\frac{(\rho-\rho_o)}{\rho_o}=\frac{3}{4}\lambda_{50}$$

Dividing the second expression by the first, we obtain

$$\frac{B_{50}}{B} = \frac{\lambda_{50}}{\lambda} = \frac{w^2}{w_{50}^2} = \left(\frac{w}{w_{50}}\right)^2 \tag{5}$$

It follows that the square of the ratio of the flow velocity and the hovering velocity defines the state of equal recovery of different particulate fractions. As is shown by the experimental results, for turbulent flows this parameter is universally valid. For such flows, as is known, the coefficient of particle resistance does not depend on the value of Re.

3. SEPARATION IN LAMINAR AND TRANSITIONAL REGIMES

Laminar and transitional regimes are characteristic of classification along small particle size boundaries. In this respect, this kind of air classification is closer to separation in liquids, where the medium flows past the particles in what are essentially non-turbulent regimes.

The material chosen in our experiments in these regimes was aluminium powder ($\rho = 2700\,\mathrm{kg/m^3}$) used in the manufacture of paints. The grain-size distribution of the powder in terms of successive residues is presented in Table II.

The experiments were carried out in a cascading air classifier comprising nine shelves with inlet at mid-height ($z = 9$; $i = 5$).

Under the assumption that the laws operating in this particle size range differ from those that govern larger particles, we investigated the effect of the concentration of the material in the flow on the results of the separation. The solid phase concentrations of 2.75, 6.0, and 14.3 $\mathrm{kg/m^3}$ in the carrier medium were tested. The results of these experiments are shown in Fig. 6. As can be seen from the graph, in the particular range studied here, the influence of the concentration was marginal. The limited scatter

TABLE II Granular composition of aluminium powder (a)

Separation boundary x (mm)	*Residue* (%)
0.4	6.5
0.315	6.9
0.2	14.3
0.16	7.8
0.125	6.5
0.1	6.7
0.08	7.8
0.063	8.2
0.05	3.5
0.045	4.2
0.04	4.2
0.035	4.2
0.03	4.8
0.025	4.2
0.02	3.8
0.015	1.8
0.01	1.8
0.005	1.5
0	1.3

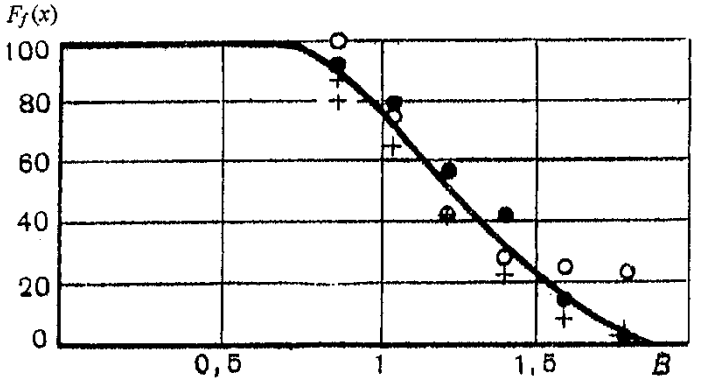

FIGURE 6 Graph of $F_f(x)=f(B)$ for different concentration of the solid particles in the carrier flow in a classifier with $z=9$, $i=5$.

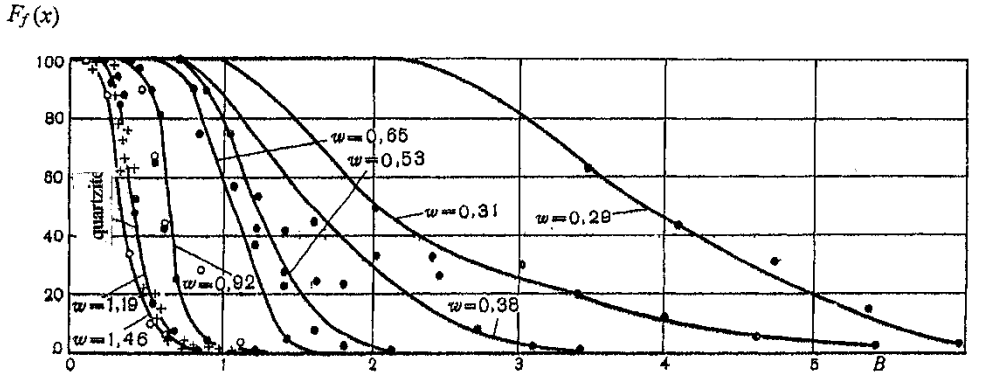

FIGURE 7 Graph of $F_f(x)=f(B)$ for the classification of aluminium powder in a classifier with $z=9$, $i=5$.

TABLE III Values of separation parameters *versus* velocity of carrier medium

Flow velocity w (m/s)	1.46	1.19	0.92	0.65	0.53	0.38	0.31	0.29
B_{50}	0.35	0.41	0.65	1.1	1.23	1.6	2.0	3.9
Re_{50}	8.14	4.76	3.28	1.99	1.21	0.54	0.33	0.26

of the experimental points is attributable to the difficulty of determining grain-size distribution in this particular size range.

In the next stage, experiments were carried out under the air flow velocities ranging from 0.3 to 1.5 m/s. Each experiment was replicated three times and the results are presented in Fig. 7. The most interesting finding was that the separation curves obtained in this set of experiments, assuming, as usual, that $F_f(x)=\phi(B)$, were not affine. At higher velocities (1.46 and 1.119 m/s), the curves practically coincided, but at lower velocities the curves diverged. It was observed that the lower the flow velocity, the greater the divergence.

The value of Re_{50} was determined for each flow velocity. The values of the relevant indices and of the flow velocity are presented in Table III.

At this point a question arises: how do these experimentally determined regularities relate to the empirical laws, arrived at earlier, for the separation of larger particles? In

order to elucidate this point, experiments were carried out in the same shelf classifier ($z=9$; $i=5$) using a quartzite powder ($\rho=2670\,\text{kg/m}^3$) with particle size range from 0.1 to 3 mm under flow velocities of 4.7, 5.57, 6.67, 7.3, and 7.89 m/s. The results of the experiments were analyzed as before and are plotted in the graph shown in Fig. 7. The experimental points referring to quartzite are designated by crosses. As can be seen from the distribution of the points, the results reveal an affine relation which matches the experimental data for the classification of aluminium powder at flow velocities of 1.46 and 1.19 m/s.

Based on the values in Table III and on these experiments, the following function was constructed:

$$B_{50} = f(\text{Re}_{50})$$

The graph of this relation is shown in Fig. 8.

This relation bears a resemblance to the well-known curve, which relates the coefficient of resistance of a single particle to the Reynolds number Re:

$$\lambda = f(\text{Re})$$

Thus a clear-cut and physically sound analogy has been established between the generalized parameter B_{50} and the coefficient of resistance of particles.

At large values of Re_{50}, the parameter B_{50} has a constant value (self-similar region). This region corresponds to the turbulent interaction between the particles and the flow. On transition to laminar flow, according to Fig. 8, self-similarity breaks down and the parameters are no longer affine.

Here another interesting point arises. All the separation curves for the different regimes of flow were obtained using the same classifier. It is reasonable to assume

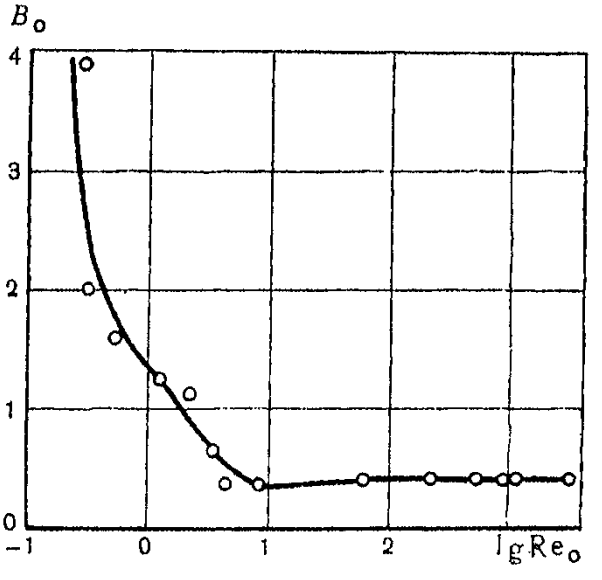

FIGURE 8 Graph of $B_{50}=f(\text{Re}_{50})$ in the overall range of separation in a classifier with $z=9$, $i=5$.

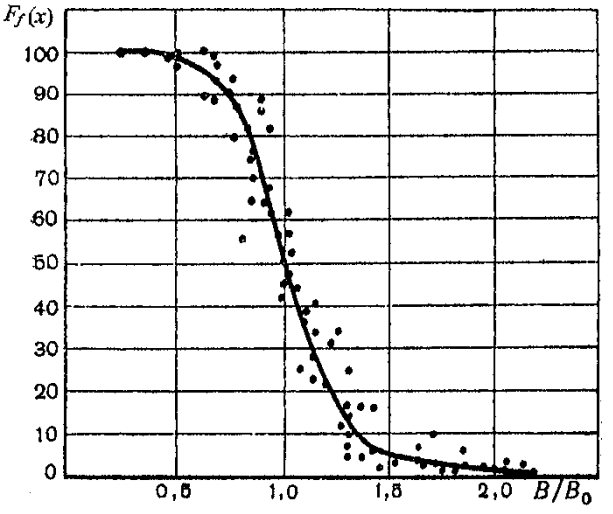

FIGURE 9 Graph of the affine relation $F_f(x)=f(B/B_0)$ for the classification of various materials in a classifier with $z=9$, $i=5$.

that there is some kind of other internal relation linking them together. To clarify this relation, we first determined the value of B_{50} for all the curves in Fig. 7. Next, for each curve, the value of the abscissa was multiplied by the reciprocal value of its own B_{50}. In general case, transformed relationship is of the form

$$F_f(x) = \psi\left(\frac{B}{B_{50}}\right) \tag{6}$$

Based on the experimental data presented in Fig. 7, we arrived at the graph shown in Fig. 9. This means that in the entire size range, and under all regimes of motion of the medium, Eq. (6) is affine.

4. CONCLUSION

We have uncovered a general empirical law governing the process of separation in the particle size range from 10 μm to10 mm. Using universal curves, it is possible to perform prognostic calculations of the separation process and compare the efficacy of different classifiers. This possibility will undoubtedly contribute to advancing the development of the technology for the separation of pourable materials.

References

[1] J. Rittinger, *Jahrbuch der Aufberietungskunge*, 1867.
[2] A.S. Monin and A.M. Yaglom, *Statistical Hydromechanics*, Parts I and II, Nauka, Moscow (in Russian), 1965 and 1967.
[3] M.D. Barsky, *Classification of Powders*, Nedra, Moscow (in Russian), 1980.
[4] E. Barsky and M. Buikis, Mathematical model for gravitational cascade separation of pourable materials at identical stages of a classifier, In: *Progress in Industrial Mathematics*, Springer Verlag, New York, 2004, pp. 229–233.

BIOGRAPHIES

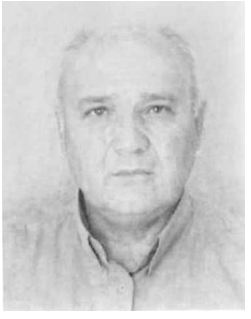

Michael Barsky was born in 1936. He graduated in Mechanical Engineering from the Ural State Technical University of Katerinburg, Russia in 1960. He received his Ph.D. degree in 1964 and D.Sc. degree in 1971. In 1973 he was appointed the full professor. In 1990, he joined the staff of Ben-Gurion University of the Negev, Beer-Sheva, Israel. Professor Barsky's scientific interests lie in mass processes, separation of free-flowing materials in air and gaseous streams, dynamics of two-phase flows in critical regimes, and physical foundations of flows of this type. Professor Barsky is the author of three books and of more than 200 scientific papers.

Eugene Barsky was born in 1974. He graduated in 1993 from Ben-Gurion University Beer-Sheva, Israel, with a B.Sc. degree in mathematics. Thereafter, he received his M.Sc. degree in 1998 and Ph.D. degree in 2001 in Industrial Mathematics. In 2002, he became a staff member of the Negev Academic College of Engineering, Beer-Sheva, Israel. His scientific interests lie in the mathematical modelling of technological processes, optimization and combinatorics. Dr. Barsky has published 15 articles.